

Evaluation of Air Flow Characteristics of Aerostatic Thrust Porous Bearings: A Numerical Approach



Marcelo Gustavo Coelho Resende¹, Leandro José da Silva¹, Cláudio de Castro Pellegrini² and Túlio Hallak Panzera^{1*}

¹Centre for Innovation and Technology in Composite Materials (CITeC), Federal University of São João del-Rei (UFSJ), Brazil

²Department of Thermal and Fluid Sciences (DCTEF), Federal University of São João del-Rei (UFSJ), Brazil

*Corresponding author: Túlio Hallak Panzera, Centre for Innovation and Technology in Composite Materials (CITeC), Federal University of São João del-Rei (UFSJ), Praca Frei Orlando 170, São João del-Rei, Brazil

Submission: 📅 September 12, 2018; Published: 📅 October 24, 2018

Abstract

Aerostatic porous bearings have been investigated in the last decades for precision engineering designs, since these bearings offer zero-friction and high operating speeds, as well as providing a very precise positioning system without external influence. Numerical methods such as CFD (Computational Fluid Dynamics) play an important role in the design and behaviour analysis of porous aerostatic bearings, being possible to adjust the geometry and characteristics of the porous restrictor even before its manufacture. In the present work, the behaviour of the gas at the inlet and outlet of a porous thrust bearing made of cementitious composites is analysed by numerical simulation using CFD method. The results reveal a stable behaviour of the cementitious porous bearing and a good correlation between numerical and experimental load capacities.

Keywords: Aerostatic thrust bearing; Porous restrictor; CFD; numerical simulation; Cementitious composites

Introduction

Aerostatic bearings have a gas flow restrictor that creates a thin film between two surfaces in relative movement, thus promoting near zero-friction. They are classified as “orifice” or “porous” medium types. The porous medium type has the potential to generate a more uniform pressure distribution in the bearing gap, relative to the orifice aerostatic bearing. In this manner, the porous bearing may provide enhanced stiffness and damping characteristics [1-3]. The most widespread application of aerostatic bearings is in the ultra-precision transformation industry, in which rigidity and stability play a key role in achieving movement accuracy. High precision milling machines require rigidity and low vibration for high speed jobs. The vibration of the tool has a significant influence on the machining accuracy. In these applications, the use of aerostatic bearings with porous restrictors is most advisable [4-8].

The effects of the geometry and operational parameters of aerostatic bearings on their performance can be evaluated using numerical simulation, such as Computational Fluid Dynamics (CFD). Important parameters include the physical and mechanical properties of the porous medium, such as porous pad geometry, diffuser angle, loading, pressure and gas flow rate, among others. Approximate solutions produced by CFD are obtained by solving iteratively a set of conservative equations applied to defined elementary volumes, that is, the control volumes [9]. The use of computational analysis and approximate methods to predict the behaviour of complex systems is important because of the difficulties involved in obtaining closed analytical solutions and conducting reliable experiments. This can considerably reduce the project costs [10].

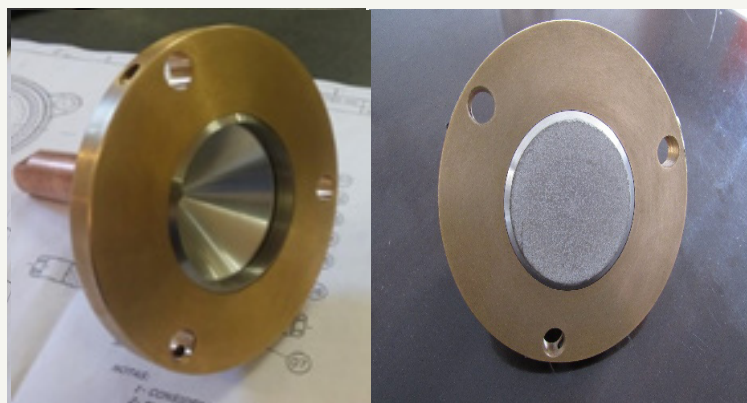


Figure 1: Aerostatic thrust bearing with cementitious porous medium.

In this work, a new model of aerostatic bearing (Figure 1) is studied through numerical simulation. The boundary conditions are considered to analyse the air flow characteristics at the inlet and outlet of the porous cementitious thrust bearing. In addition, a comparison between the bearing load capacity obtained through numerical simulation and experimentally is presented.

Methodology

Figure 2 shows the bearing prototype proposed in this work. It consists of a cylindrical inlet (4.2 mm in diameter), a diffuser and the porous restrictor (50mm in diameter and 8 mm thick). The porous restrictor was proposed by Panzera et al. [11], being designed based

on a cementitious composite reinforced with silica microparticles via cold uniaxial pressing. This composite reaches 30% of porosity and $1.14 \times 10^{-15} \text{m}^2$ of viscous permeability coefficient.

In most precision engineering applications, the bearing gaps (air film thickness) range from 5 to 20µm. It is well known that lower values of thickness provide lower gas consumption and higher stiffness [1-3]. However, in the simulation process, a smaller region of analysis requires a refined mesh. In order to reduce computer time a thicker bearing gap of 20µm was considered. The flow rate used in the numerical experiment was 2.104 ml.s^{-1} . This value was determined experimentally using the bearing shown in Figure 1.

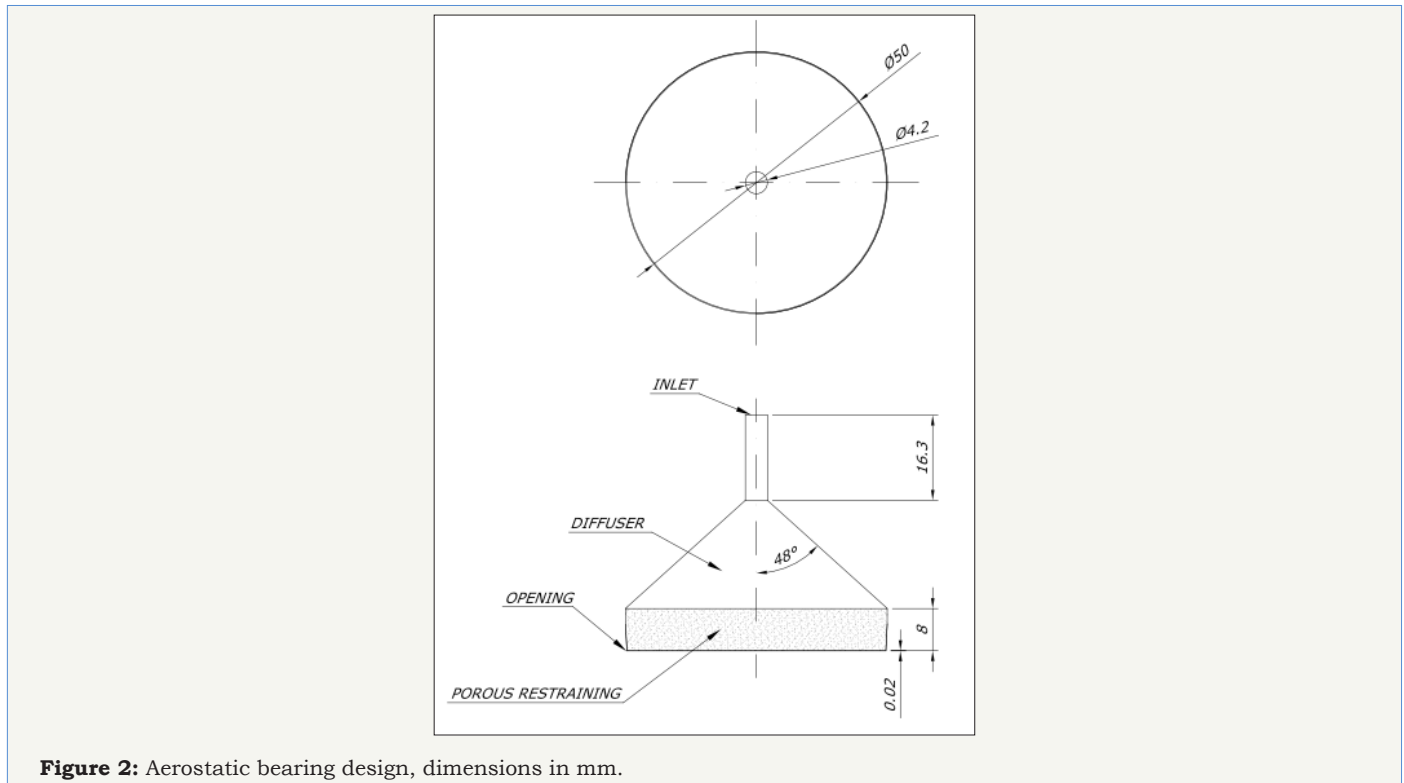


Figure 2: Aerostatic bearing design, dimensions in mm.

The CFD analysis was performed based on a static model (Figure 2), i.e., the bearing is not able to rotate and translate in radial and axial directions. In addition, the inlet gas velocity (axial direction),

the outlet gas pressure (radial direction of the restrictor), the input data and the bearing geometry were maintained constant.

Table 1: Contour conditions and domain data.

| Material | Model |
|---------------|---|
| Ideal gas-Air | Heat transfer model=Thermal energy |
| | Turbulence model=SST (Shear Stress Transport) |
| | Turbulent wall functions=automatic |
| | Buoyancy model=non-buoyant |
| | Domain motion=stationary |
| | Reference pressure=1atm |

Table 1 exhibits the mathematical models and conditions imposed to solve the problem. For the simulation, the air was considered an ideal gas. The effects of gravitational force on the gas flow were disregarded and the domain was established as stationary. The SST (Shear Stress Transport) two-equation turbulence model

was used in this work. This model is considered robust and is widely used in aerodynamic applications [12]. It uses the K-omega model in the inner boundary layer and K-epsilon in the free-flow shear (Table 2).

Table 2: Contour conditions and data of surfaces and boundaries.

| Local | Type | Configuration |
|--------|---------|---|
| Input | Inlet | Flow regime=Subsonic |
| | | Mass and momentum=Normal speed; 2.1m/s |
| | | Turbulence=Medium (Intensity=5%) |
| | | Heat transfer=Static temperature; 293K |
| Output | Opening | Flow regime=Subsonic |
| | | Mass and momentum=Opening pressure: 0atm |
| | | Flow direction=Normal to boundary condition |
| | | Turbulence=Medium (Intensity=5%) |
| | | Heat transfer=Opening temperature; 293K |
| Wall | Wall | Mass and momentum=No slip wall |
| | | Wall roughness=Smooth wall |
| | | Heat transfer=Adiabatic |

Table 3 shows the characteristics used for the domain of the porous restrictor. The properties of the porous pad were obtained from Panzera et al. [11]. The interface regions that characterise the air flow and the relationship between the fluid and porous domains have been established for the contacts between the diffuser and the restrictor, and between the restrictor and the bearing gap.

Table 3: Properties of the porous restrictor used.

| Material | Model |
|--|--|
| Cementitious composite reinforced with silica microparticles | Area porosity=Isotropic |
| | Volume porosity=0.3 |
| | Loss model=Isotropic loss |
| | Loss velocity type=Superficial |
| | Isotropic loss=Permeability and loss coefficient |
| | Permeability=1.14e-15 [m ²] |
| | Fluid solid area density=Interfacial area density |
| | Interfacial area Den.=0.001[m ⁻¹] |
| | Fluid solid heat transfer=Heat transfer coefficient |
| | Heat transf. coeff. 1[Wm ⁻² K ⁻¹] |
| | Reference pressure=1atm |

A three-dimensional mesh containing tetrahedral and prismatic elements was used. A convergence test was performed for the mesh configuration, attempting successive reductions in element size until no significant difference in results is achieved.

Results

Figure 3 shows the streamlines configuration of the airflow through the diffuser and the porous medium. A toroidal vortex can be observed in the diffuser, alongside a main jet. It appears due to the rapid increase in the area of the diffuser that causes a decrease in velocity and therefore an increase in pressure. On the other hand, the porous restrictor presents laminar flow, exhibiting a nearly uniform distribution of airflow in the bearing gap.

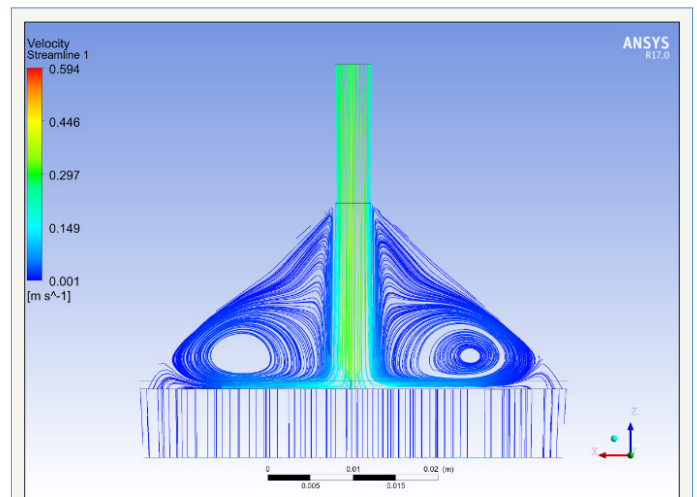


Figure 3: Velocity result with the streamline.

Figure 4 shows the pressure distribution in the air gap. The pressure profile is important because it allows the occurrence of pneumatic instability (due to the asymmetry and magnitude of the pressure distribution) to be observed. It can be seen in Fig. 4 that the pressure distribution is symmetric and uniform, with a smooth decay at the ends, indicating a stable behaviour for the bearing studied.

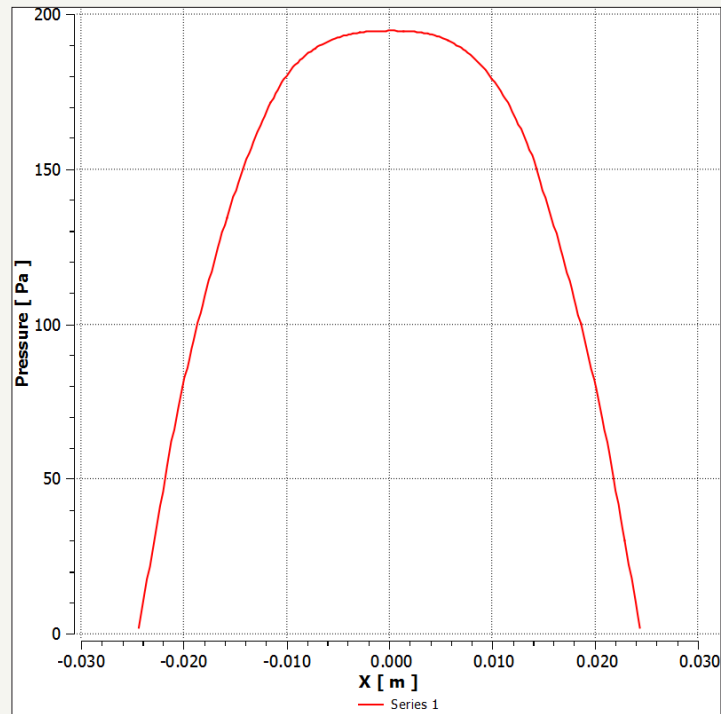


Figure 4: Profile pressure in the air gap region.

The load capacity of the air bearing can be obtained by integrating the simulated pressure along the surface area of the restrictor. Based on the pressure distribution shown in Figure 4, a

load capacity of 7.23 N was calculated, fitting well with the bearing weight shown in Fig. 1, 7.46 N (a 3% difference).

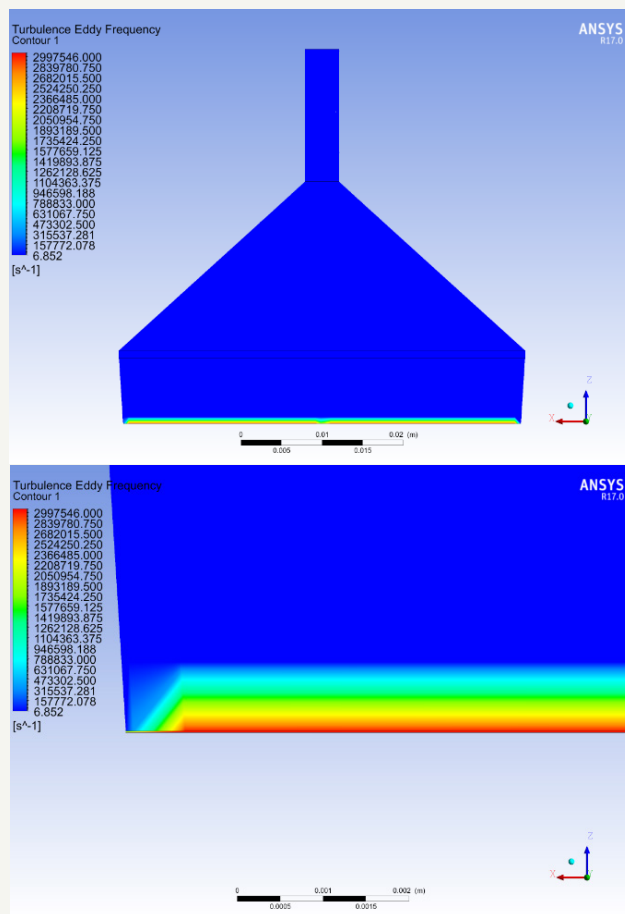


Figure 5: Distribution of the frequency of turbulence.

Figure 5 shows the simulated turbulence eddy frequency in the aerostatic bearing. This information is also important to verify the existence of resonance and consequently of pneumatic instability. The results reveal a higher frequency in the air gap region, especially in the central portion of the outlet surface of the porous restrictor.

Conclusion

The numerical simulation proposed in this work estimated the characteristics of the airflow within the aerostatic bearing, the distribution of the air pressure in the bearing gap, the stability and load capacity of the bearing. A toroidal vortex formation was observed in the diffuser; however, a laminar airflow through the porous restrictor was observed in the simulation, suggesting a stable behaviour for the cementitious bearing. These results corroborate the development of the design of the aerostatic thrust bearing, which will be the scope of future investigations.

Acknowledgment

The authors would like to thank CAPES, and CNPq (MCTI/CNPq no. 01/2016) for the financial support provided.

References

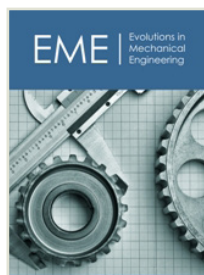
- Kwan YBP, Corbett J (1998) Porous aerostatic bearing-an updated review. *Wear* 222: 69-73.
- Silva LJ, Panzera TH, Viera LMG, Bowen CR, Duduch JG, et al. (2018) Cementitious porous material applied to precision aerostatics bearings. *International Journal of Precision Engineering and Manufacturing* 19(2): 239-243.
- Silva LJ, Panzera TH, Viera LMG, Bowen CR, Duduch JG, et al. (2017) Carbon nanotubes and superplasticizer reinforcing cementitious composite for aerostatic porous bearing. *Proceedings of the Institution of Mechanical Engineers, Part J, Journal of Engineering Tribology* 231(11): 1397-1407.
- Huo D, Cheng K, Wardle F (2010) Design of a 5-axis ltraprecision micro milling machine-ultramill: part 1: holistic design approach, design considerations, and specifications. *International Journal of Advanced Manufacturing Technology* 47(9): 867-877.
- Gao SY, Cheng K, Ding H (2016) Multiphysics-based design and analysis of the high-speed aerostatic spindle with application to micro-milling. *Proceedings of the IMechE, Part J: Journal of Engineering Tribology* 230(7): 852-871.
- Yuan JL, Zhang FH, Dai YF, Kang R, Yang H, et al. (2010) Development research of science and technologies in ultra-precision machining field. *Chinese Journal of Mechanical Engineering* 46(8): 161-177.
- Wang W, Jiang Z, Tao W, Zhuang W (2015) A new test part to identify performance of five-axis machine tool-part I: geometrical and kinematic characteristics of S part. *International Journal of Advanced Manufacturing Technology* 79(5-8): 1-10.
- An C, Zhang Y, Xu Q, Zhang FH, Zhang JF, et al. (2010) Modeling of dynamic characteristic of the aerostatic bearing spindle in an ultra-precision fly cutting machine. *International Journal of Machine Tools and Manufacture* 50(4): 374-385.
- Cui H, Wang Y, Yue X, Huang M, Wang W (2017) Effects of manufacturing errors on the static characteristics of aerostatic journal bearing with porous restrictor. *Tribology International* 115: 246-260.
- Pinto RN, Afzal A, D'souza LV, Ansari Z, Mohammed Samee AD (2017) Computational fluid dynamics in turbomachinery: a review of state of the art. *Archives of Computational Methods in Engineering* 24(3): 467-479.
- Panzera TH, Rubio JCC, Bowen C, Walker P (2008) Microstructural design of materials for aerostatic bearings. *Cement & Concrete Composites* 30(7): 649-660.
- Neves MT, Schwarz VA, Menon GJ (2007) Analysis of externally pressurized gas journal bearing by using the finite element method. In: 19th International Congress of Mechanical Engineering, Brasilia. *Proceedings of COBEM2007* ID code: 2173.



Creative Commons Attribution 4.0 International License

For possible submissions Click Here

Submit Article



Evolutions in Mechanical Engineering

Benefits of Publishing with us

- High-level peer review and editorial services
- Freely accessible online immediately upon publication
- Authors retain the copyright to their work
- Licensing it under a Creative Commons license
- Visibility through different online platforms